Z. Phys. Chem. **225** (2011) 913–926 / **DOI** 10.1524/zpch.2011.0125

OH and NH Stretching Vibrational Relaxation of Liquid Ethanolamine

By Stephan Knop, Jörg Lindner, and Peter Vöhringer*

Lehrstuhl für Molekulare Physikalische Chemie, Institut für Physikalische und Theoretische Chemie, Rheinische Friedrich-Wilhelms-Universität Bonn, Wegelerstraße 12, 53115 Bonn, Germany

Dedicated to Prof. Horst Hippler on the occasion of his 65th birthday

(Received April 12, 2011; accepted in revised form May 30, 2011)

Vibrational Relaxation / Liquid Dynamics / Hydrogen-Bonding / Ultrafast Spectroscopy

Femtosecond mid-infrared pump-probe spectroscopy was carried out to obtain information about the dynamics of vibrational energy relaxation in liquid ethanolamine at room temperature and ambient pressure. Through partial deuteration it was possible to disentangle the dynamics resulting from the OH and the NH stretching modes that proceed independently and simultaneously in the hydrogen-bonded liquid following an ultrafast vibrational excitation by a resonant mid-infrared pulse. The OH-stretching vibrational lifetime was determined to be 450 fs while the NH-stretching lifetime was found to be 1.2 ps. This large difference in lifetimes highlights the importance of the hydrogen-donating and the hydrogen-accepting character of the vibrating groups that are engaged in hydrogen-bonding.

1. Introduction

Vibrational energy relaxation (VER) in molecular liquids has attracted considerable attention of researchers devoted to exploring condensed phase chemical dynamics. Associated molecular liquids have been particularly attractive research targets because the influence of hydrogen bonding (H-bonding) on the timescales and molecular mechanisms of the various vibrational dynamical phenomena remains until today only partially understood [1–3].

Naturally, the most comprehensively studied system is pure liquid water [4–7]. Its vibrational relaxation dynamics following an initial OH-stretching excitation has been studied extensively by femtosecond (fs) time-resolved mid-infrared (MIR) spectroscopy. Immediately after laser-excitation of the $v = 0$ to $v = 1$ transition of the OH-stretching mode, the excess energy rapidly delocalizes onto neighboring water molecules thereby giving rise to an ultrafast loss of memory regarding the frequency of excitation as well as the orientation of the associated transition dipole [8–10]. These

* Corresponding author. E-mail: p.voehringer@uni-bonn.de

dynamics are facilitated by strong OH transition dipole interactions, *i.e.* excitonic coupling, which was recently mimicked more clearly in synthetic low-dimensional periodic model systems exhibiting spatially extended H-bond patterns that are structurally more ordered than the stochastic H-bond networks of bulk water [11,12].

A further complication arises in neat H_2O from the Fermi resonance between the OH-stretching fundamental and the first overtone of the bending vibration. This additional complexity can be lifted by studying the monodeuterated isotopomeric systems HOD dissolved in H_2O or in D_2O, respectively [13–19]. Furthermore, in these systems the OH (or OD) vibrator finds itself highly diluted in a bath consisting exclusively of OD (or OH) oscillators. This deuteration also circumvents a canonical heating of the sample that will inevitably occur upon laser induced vibrational excitation of the neat liquid. Depopulation of the $v = 1$ vibrational state occurs on a time scale of about 1 ps and is believed to occur through the bending manifold [5,14,18,20–24].

Any energy mismatch that may arise from a transition between an upper and a lower vibrational state has to be compensated for by the low-frequency phonon modes of the liquid [25]. The phonon-spectral density of liquid water is highly unique due to the existence of the extended random H-bond network [26,27]. Apart from overdamped and diffusive contributions [28], it essentially consists of three broad intermolecular vibrational bands originating from the three quasi-degenerate restricted rotational modes (*i.e.* librations) and the two restricted translational degrees of freedom that are directed parallel and perpendicular to H-bonds between nearest neighbor molecules [26,27]. Thus, the phonon spectral density of liquid water has substantial amplitude up to about $1000\,\mathrm{cm}^{-1}$ extending almost into the intramolecular vibrational region. In addition to the strong intermolecular couplings, this explains the ultrafast nature of the vibrational relaxation dynamics in water as compared to those of nonpolar liquids. A similarly VER is observed for water when the fundamental transition of the bending vibration, the bending vibrational combination tone or the librational fundamental is excited [5,21–23].

Finally, a systematic study of the temperature and density dependence of the VER dynamics from liquid to supercritical water reveals a fascinating new physicochemical anomaly, namely an increase of the VER rate with decreasing temperature [17,18]. This behavior is even more surprising in light of the finding that the pure density dependence of the isothermal VER rate is exceptionally well reproduced by a simple description invoking isolated binary collisions (IBC) between attractive hard sphere molecules [18]. Such a model would in turn predict an increase of the VER rate with temperature as the average particle velocities and hence, the collision frequencies increase. Complementary studies of these dynamics of liquid-to-supercritical ammonia do indeed show an increase of the VER rates with both, the temperature and the density, which is fully captured by the IBC model [29].

Of course, hydrogen-bonding and the intermolecular couplings are considerably weaker in liquid ammonia as compared to liquid water and consequently, the ND-stretching relaxation of NH_2D in NH_3 is slower as compared to the corresponding OD-stretching relaxation of HOD in H_2O [29]. However, whereas hydroxyl groups are known to be better H-bond donors as amino groups, they are inferior H-bond acceptors. Therefore, it would be interesting to study the VER dynamics of liquids featuring both, a very good H-bond donor such as an OH group and a strong H-bond acceptor such

as an amino group. The simplest model system of such kind is hydroxyl amine. However, NH_2OH is a crystalline solid that tends to decompose explosively into ammonia, dinitrogen, and water at room temperature and is therefore not a feasible molecule to such experiments. Alternatively, one can resort to amino alcohols, the simplest of which – aminomethanol – is only available as a stabilized ammonium chloride and therefore neither a suitable system. In contrast, aminoethanol (or ethanolamine, EA) is readily available as a neat viscous liquid with normal freezing and boiling point of 10 °C and 172 °C [30]. To our knowledge femtosecond spectroscopic experiments on the VER dynamics of liquid EA in the mid-infrared have not been carried out yet. Only molecular dynamics (MD) calculations have been conducted for this system to characterize the thermodynamics, in particular the liquid-vapor coexistence [31], the surface tension [31], and the local solvation structure with an emphasis on the hydrogen bonding properties [32–34]. Da Silva *et al.* developed a force field for EA from electronic structure calculation based on density functional theory [33]. Their MD simulations was analyzed in terms of conformer distribution, which seemed to suggest that the carbon-carbon dihedral angle tends to adopt a gauche conformation so as to facilitate significant intramolecular hydrogen-bonding in addition to H-bonding to nearest neighbors as is typical for liquid water or for liquid alcohols.

In this paper, we will report first MIR pump-probe experiments on the vibrational relaxation dynamics of liquid EA at room temperature and ambient pressure. Our data enable the extraction of the individual VER rates related to the decay of an initially deposited NH-stretching and OH-stretching quantum. It turns out, that the OH-stretching relaxation is about a factor of three faster than the NH-relaxation, which implies that hydrogen-bond donation is of greater importance to vibrational energy relaxation than H-bond acceptance.

2. Experimental

Femtosecond mid-infrared pump-probe spectroscopy was carried out using a pair of independently tunable optical parametric amplifiers (OPA) that was synchronously driven at a repetition rate of 1 kHz by the optical pulses (200 fs duration, 800 μJ energy) of a frequency-doubled Erbium fiber oscillator/Ti:sapphire chirped pulse regenerative amplifier. Each OPA was equipped with a difference frequency generator (DFG) based on $AgGaS_2$. One of the OPA/DFG units served as the source for the excitation pulses while the other one was used to generate detection pulses. These in turn were divided into probe and reference pulses by a 50% beamsplitter. The pump pulses were steered through a computer controlled translation stage to adjust their relative timing to the probe pulses. The relative polarization between the pump and probe pulses was set to the magic angle using a half-wave retardation plate. The pump and probe pulses were then spatially overlapped in the liquid sample using an Au-coated off-axis parabolic mirror (OAP) with an effective focal length of 10 cm. An identical OAP was used to collimate the beams behind the sample and the pump light was blocked by a beam dump to suppress residual pump scatter. The probe and reference pulses were then focused onto the entrance slit of an 0.2 m monochromator, whose exit slit was replaced by a 2×32 pixel HgCdTe array detector thereby enabling the measurement of

the pump-induced optical density in a frequency-resolved reference detection scheme with a spectral resolution of 20 cm^{-1}. Typically, the pump-induced optical density was obtained by averaging over 1000 laser pulses. The liquid samples were contained in an optical cell (path length 50 μm) that was sealed with CaF_2 windows. Typical optical densities of the samples at the pump frequency were 0.3. There was no indication for thermal lensing effects despite using a non-rotating or non-flowing sample.

Liquid ethanolamine (EA, purified by redistillation, ≥ 99.5%) was purchased from Sigma Aldrich and was used without further purification. Deuterium oxide (D_2O) was purchased from Eurisotop and had an isotopic purity of 99.9%. Ethanolamine-d3 ($D_2NCH_2CH_2OD$) was prepared by mixing 2 mL of D_2O with 0.5 mL of EA in a nitrogen atmosphere. The solution was destilled at a pressure of 100 mbar and a temperature of 45 °C to remove the D_2O/HOD mixture from the partially deuterated EA. The isotopic purity was checked for by means of Fourier transform infrared (FTIR) spectroscopy.

3. Results and discussion

In the gas phase and in non-polar weakly interacting solvents, ethanolamine molecules can adopt various conformations resulting in intramolecularly hydrogen-bonded and non-bonded amino and hydroxyl groups that are spectroscopically distinguishable [35–37]. An IR spectrum recorded in the gas phase therefore features a number of absorption bands between 3550 and 3670 cm^{-1} that are assigned to the "free" and the "bound" OH-groups of these various conformers. In addition, NH-stretching absorptions were identified around 3420 cm^{-1} [35–37].

A Fourier transform infrared spectrum (FTIR) emphasizing the entire stretching spectral region of liquid ethanolamine from 2500 to 3500 cm^{-1} is displayed in Fig. 1a. Apart from the two CH-stretching bands at 2864 and 2931 cm^{-1} the complexity of the vibrational spectrum is much reduced as compared to the gas phase. The symmetric and antisymmetric NH_2-stretching fundamentals can be identified at 3290 and 3354 cm^{-1} whereas the single OH-stretching fundamental is now located at 3180 cm^{-1}. The pronounced shift of all these transitions to lower frequencies relative to the gas phase is indicative of the formation of hydrogen-bonds in the liquid phase [38] that are of intermolecular nature and thus, much stronger than the intramolecular hydrogen-bonded contacts identified in the gas phase. Also, free hydroxyl and amino vibrators can no longer be differentiated as all OH and NH groups are fully engaged in forming an extended H-bond network.

Figure 1a also demonstrates that the OH and NH vibrational resonances strongly overlap. Therefore, it is practically impossible to excite them individually with a femtosecond MIR pulse, which precludes an independent determination of the NH and OH stretching vibrational relaxation rates from a time-resolved pump-probe experiment. We can avoid this ambiguity again through a partial deuteration. A solution of 4% ethanolamine in ethanolamine-d3 exhibits an FTIR spectrum that is shown in Fig. 1b. At such a low mixing ratios, the probability for finding two hydrogen atoms on the hydroxyl and/or amino groups of the same single ethanolamine molecule is negligible. Basically, for frequencies higher than 3000 cm^{-1}, the spectrum shown in

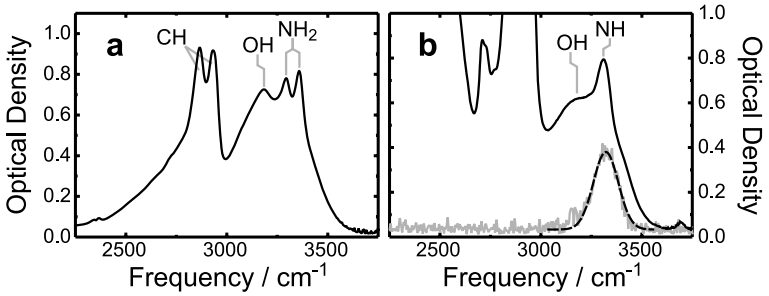

Fig. 1. FTIR spectrum of neat liquid ethanolamine (**a**) and of a solution of 4% ethanolamine in ethanolamine-d3 (**b**). Both spectra were recorded at room temperature and ambient pressure. The spectrum of the excitation pulses used for the pump-probe experiments is shown in (**b**) in gray together with a Gaussian fit (dashed).

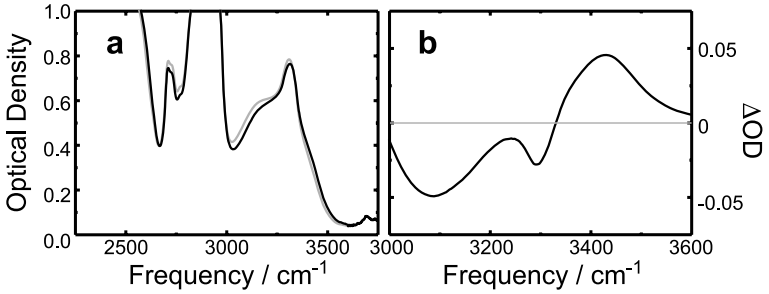

Fig. 2. (**a**) FTIR spectra of a solution of 4% ethanolamine in ethanolamine-d3 at 295 K (gray) and at 315 K (black). (**b**) Thermal difference spectrum (focusing on the OH/NH resonance only) obtained by subtracting the two spectra shown in (**a**). A negative differential optical density corresponds to a bleach while a positive ΔOD represents an induced absorption.

Fig. 1b is brought about by two independent species namely, $D_2NCH_2CH_2OH$ and $HDNCH_2CH_2OD$, which we abbreviate as EA-OH and EA-NH. Both of these species are highly diluted in a bath consisting of ethanolamine-d3, *i.e.* $ND_2CH_2CH_2OD$.

This expectation is fully confirmed by the finding that the partial deuteration destroys the symmetric–asymmetric splitting of the NH-stretching resonance of neat fully hydrogenated ethanolamine thereby collapsing into a single NH-absorption band at 3309 cm^{-1}. This feature originates exclusively from the EA-NH species and is superimposed on a single broad absorption band originating from the hydroxyl group of the EA-OH species.

For an analysis of time-resolved MIR pump-probe experiments it is also advantageous to have information regarding the temperature-dependence of the linear absorption spectrum [12]. Figure 2a shows FTIR spectra of a 4% solution of EA in EA-d3 recorded at two different temperatures (22 °C to 42 °C) from which a thermal difference spectrum, ΔOD, can be computed. The latter is reproduced in Fig. 2b. As can be seen, the temperature jump gives rise to a slight shift of the overall OH/NH-resonance to higher frequencies thereby resulting in a positive differential optical density, *i.e.*

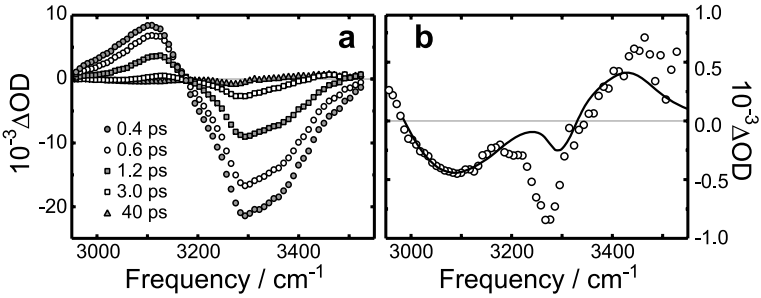

Fig. 3. (**a**) Transient differential spectra for a few representative pump-probe delays of a 4% solution of ethanolamine in ethanolamine-d3 at room temperature and ambient pressure following an initial NH/OH-stretching excitation. (**b**) Comparison of the pump-induced spectrum at a delay of 40 ps with a thermal difference spectrum. The latter was scaled by a factor of 1/90.

in an induced absorption, for frequencies higher than 3330 cm^{-1} while for lower frequencies, ΔOD is negative corresponding to an induced bleach. The intermediate, negative going peak at 3296 cm^{-1} is very close to the linear NH-stretching resonance and seems to originate solely from bleaching of the vibrational ground state of the EA-NH species.

The spectral position of high-frequency oscillators (such as OH and NH groups) engaged in hydrogen-bonding are known to correlate very well with the local hydrogen-bond geometry, *i.e.* with the H-bond length [7,38,39] and angle [7,39]. The blue shift seen in Fig. 2 is highly reminiscent of the thermally induced blue-shift of the OH resonance reported previously for liquid water and indicates an on-average lengthening and weakening of the hydrogen-bonds upon increasing the temperature [38].

Having characterized the stationary spectroscopy of the two coexisting monodeuterated ethanolamine molecules, we now turn our attention to its dynamic MIR OH/NH stretching response following a femtosecond fundamental OH/NH stretching excitation. Figure 3a reproduces representative pump-induced differential spectra of a 4% solution of EA in EA-d3 obtained by exciting the solution with a pump pulse whose spectrum was tuned to the maximum of the OH/NH stretching band (*cf*. also Fig. 2).

The data display two distinct regions, an induced bleach and an induced absorption, which are separated by an apparent isosbestic frequency of 3200 cm^{-1}. At zero time delay, the fundamental $v = 0$ to $v = 1$ transitions of the OH and NH stretching modes of the two species, EA-OH and EA-NH, are excited. This depletes the vibrational ground states of the two molecules and leads to a diminished absorption at the pump frequency (3300 cm^{-1}), *i.e.* the ground state holes. At the same time, since the $v = 1$ excited vibrational states are populated, stimulated emissions to the stretching mode ground states of the two species can occur. These two stimulated emissions are spectroscopically indistinguishable from the two ground state holes. Together, these four induced transitions (one ground state hole and one stimulated emission for each independent species) contribute to the negative differential optical density seen in Fig. 3 for probe frequencies above 3200 cm^{-1}.

The transient population in the stretching excited state also allow for absorptive transitions to their respective next higher lying vibrational state. However, since the

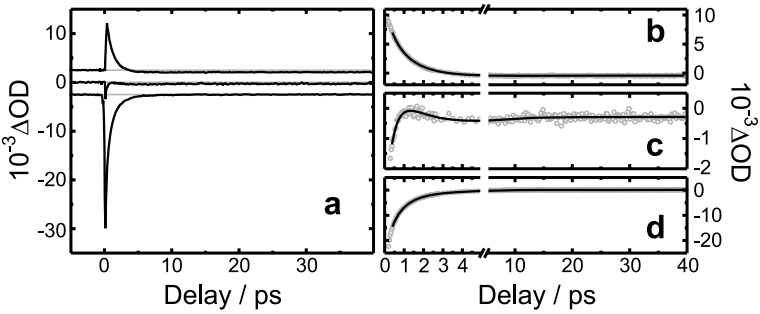

Fig. 4. (**a**) Femtosecond MIR pump-probe traces of a 4% solution of ethanolamine in ethanolamine-d3 at room temperature and ambient pressure for three representative detection frequencies following an initial NH/OH-stretching excitation. The traces have been shifted vertically by 2.5 mΔOD. The probe frequencies are 3116, 3186, and 3279 cm^{-1} (from top to bottom). (**b**)–(**d**) Comparison of the experimental data with triple-exponential fits (see text for details) for probing at 3116 cm^{-1} (**b**), 3186 cm^{-1} (**c**), and 3279 cm^{-1} (**d**). Note the break in the time delay axis.

stretching modes are intrinsically anharmonic in character, the transitions from $v = 1$ to $v = 2$ are shifted to lower frequencies relative to their corresponding fundamentals. These two anharmonically shifted transient absorptions (one for each species) contribute to the positive differential optical density seen in Fig. 3 for probe frequencies below 3200 cm^{-1}.

Since in the harmonic approximation the square of the matrix elements, $\langle v|\,\hat{\mu}\,|\,v+1\rangle$, of the vibrational transition dipole operator, $\hat{\mu}$, are proportional to the quantum number, v, the transient absorption ($v = 1$, $v+1 = 2$) is expected to be roughly equal in magnitude as the sum of the ground state hole and the stimulated emission ($v = 0$, $v+1 = 1$, for both). However, the two signal amplitudes differ by about a factor of two, which is simply to large to be rationalized by the anharmonicity of the two stretching modes. It could very well be that the spatial overlap of the pump and the probe pulses inside the liquid sample was spectrally non-uniform in our experiment. Alternatively, it might also be that the high-energy wing of the overwhelming linear absorption of the CH-stretching bands (*cf*. Fig. 1b) begins to distort and attenuate the pump-induced optical densities with decreasing probe frequency.

As the delay time, t, increases, both spectral components gradually decay concertedly while more or less preserving the "isosbestic" frequency. The recovery of the induced bleach/emission and anharmonically shifted absorption is brought about by the dynamics of vibrational relaxation and the concurrent refilling of the vibrational ground state hole. From the precise temporal decay of the induced absorption and the time-dependent recovery of the fundamental transitions we can obtain information regarding the time scales and the mechanisms of VER. To this end, kinetic traces are selected in Fig. 4 for some few representative probe frequencies distributed across the entire NH/OH stretching region.

Firstly, in the bleaching/emission region (*i.e.* at a probe frequency of 3279 cm^{-1}), the signal rises instantly within the time-resolution of our experiment and subsequently decays within a time window of about 5 ps. A careful inspection of this particular trace reveals a residual (*i.e.* permanent) long term induced absorption with a magnitude of

roughly 100 μOD. Secondly, in the induced absorption region (*i.e.* at a probe frequency of 3116 cm^{-1}), the signal also appears promptly and decays again on a time scale of *ca.* 5 ps. Carefully checking this kinetic trace at very long delays discloses a permanent induced bleach having an amplitude of −400 μOD. In other words, both kinetic traces reverse their sign such that an initial absorption turns over into a bleach while an initial bleach evolves into an absorption.

The resultant differential absorbance spectrum at very long delays is displayed in Fig. 3b. The observation of an induced absorption that is "blue"-shifted relative to the stationary absorption spectrum that is accompanied by a residual "red"-shifted bleach is highly indicative of a thermally heating of the sample volume [3,12,22]. Such a heating occurs when the initially deposited OH/NH stretching energy is canonically redistributed over all nuclear (intra and intermolecular) degrees of freedom of the liquid. Similar quasi-permanent spectra were observed in femtosecond MIR spectroscopy of liquid water and its isotopomeric mixtures [3,12,17,22,40].

To test this interpretation, the long-time differential spectrum is compared in Fig. 3b with the thermal difference spectrum discussed above. A qualitative agreement between these two spectra is evident, there are however also quantitative differences. While the emissive and absorptive features and their magnitudes at the high and low frequency edges of the spectral window agree rather well, the bleaching of the narrower NH-stretching resonance is much stronger in the time-resolved experiment as compared to the thermal difference measurement. The lack of quantitative agreement is however easily rationalized by considering that the infrared NH/OH-stretching activity of the sample results from two chemically distinct and highly diluted species. It would not at all be surprising if the time scale for canonical energy randomization depends on the nature of the vibration that is initially excited by the pump pulse. If for example the NH-stretching vibrational relaxation is much slower than the OH-stretching relaxation, then the excited NH-stretching state of the EA-NH species might still be fully populated at long delays, while the EA-OH species would already be embedded in hot microscopic environment because its OH-stretching excess energy has been fully redistributed among the nuclear degrees of freedom of its immediate environment. Consequently, a bleach of the NH-stretching fundamental would be detected that is expected to be stronger than that resulting from a thermal heating.

To follow up on the notion of different time scales relevant to NH and OH-stretching vibrational relaxation, a global fitting analysis has been carried out on the probe-frequency dependent kinetic traces [12]. To this end, a triple-exponential fit according to

$$\Delta\mathrm{OD}(t,\ \tilde{\nu}) = H(\tilde{\nu}) + \sum_{i=1}^{3} A_i(\tilde{\nu})\ \exp\left(-t/\tau_i\right) \tag{1}$$

was used to model the MIR kinetic trace, $\Delta\mathrm{OD}(t,\ \tilde{\nu})$ at each probe frequency, $\tilde{\nu}$. Here, $H(\tilde{\nu})$ represents the long-time spectrum connected with the canonically heated sample as shown in Fig. 3b. The coefficients, $A_i(\tilde{\nu})$, are the probe-frequency-dependent amplitude of the exponential component associated with the global (*i.e.* frequency independent) time constant, τ_i. A total of 64 pump-probe traces were fitted in the frequency interval ranging from 2975 cm^{-1} to 3547 cm^{-1}. As demonstrated in Fig. 4b–d, a mini-

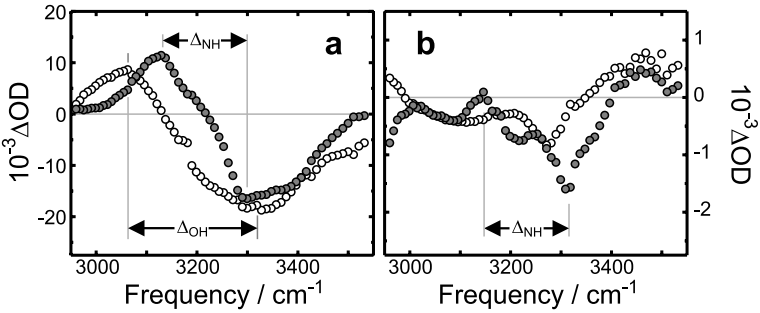

Fig. 5. Spectral amplitudes of the exponential components associated with the time constants $\tau_1 = 0.45$ ps (panel **a**, open circles), $\tau_2 = 1.2$ ps (panel **a**, filled circles), $\tau_3 = 5$ ps (panel **b**, filled circles), and the long-time spectrum from Fig. 3b multiplied by a factor of four.

mum number of three exponentials were required to obtain a satisfactory fit to all the kinetic traces simultaneously. The corresponding time constants were (0.45 ± 0.15) ps, (1.2 ± 0.3) ps, and (5 ± 3) ps. Apart from these time constants, the principal results of the fitting are the three spectral coefficients, $A_i(\tilde{\nu})$. The probe frequency dependence of these quantities is reproduced in Fig. 5.

The total MIR pump-probe response of the sample is dominated by the two fast components. The overall appearance of their spectral amplitudes, $A_1(\tilde{\nu})$ and $A_2(\tilde{\nu})$, is similar both, in terms of shape and magnitude. They are composed of a bleach/emission contribution centered around 3300 cm^{-1} and an absorptive contribution that peaks either at 3125 cm^{-1} for the 1.2-ps exponential or at 3060 cm^{-1} for the 0.45-ps exponential. Since there are two coexisting and independent species in the liquid sample that are spectroscopically distinguishable, it seems obvious to relate them to the two dominating dynamic contributions.

In a simple two-state relaxation mechanism for each of the two species, in which the excited vibrational state ($v = 1$) relaxes back to the ground state ($v = 0$), the MIR response of the EA-NH species is given by

$$\begin{aligned}\Delta\mathrm{OD}(t,\ \tilde{\nu}) = {} & n\left(|1\rangle_{\mathrm{NH}}, t=0\right)\left\{\sigma^{\mathrm{NH}}_{2\leftarrow 1}(\tilde{\nu}) - 2\sigma^{\mathrm{NH}}_{1\leftarrow 0}(\tilde{\nu})\right\}\exp\left(-t/\tau_{\mathrm{NH}}\right) \\ & + n\left(|1\rangle_{\mathrm{OH}}, t=0\right)\left\{\sigma^{\mathrm{OH}}_{2\leftarrow 1}(\tilde{\nu}) - 2\sigma^{\mathrm{OH}}_{1\leftarrow 0}(\tilde{\nu})\right\}\exp\left(-t/\tau_{\mathrm{OH}}\right) \qquad (2)\end{aligned}$$

where the NH- and OH-stretching vibrational lifetimes are given by the τ_i. For simplicity, Eq. (2) neglects any energy randomization of the NH and OH-stretching energy concomitant with a transient heating of the liquid. The number densities of the EA-NH and EA-OH molecules that are prepared by the pump pulse in the first excited NH- and OH-stretching states at zero time delay are given by $n\left(|1\rangle_{\mathrm{NH}}, t=0\right)$ and $n\left(|1\rangle_{\mathrm{OH}}, t=0\right)$. A comparison between the pump spectrum and the FTIR spectrum (see Fig. 1) of the solution suggests that the excitation probability of the two EA-NH and EA-OH species and thus, their $v = 1$ number densities, $n\left(|1\rangle_i, t=0\right)$, are about equal thereby explaining the approximately equal magnitude of the two spectral amplitudes, $A_1(\tilde{\nu})$ and $A_2(\tilde{\nu})$.

In this simple notion, the spectral amplitudes, $A_i(\tilde{\nu})$, relate directly to the difference absorption cross section, $\sigma_{2\leftarrow1}(\tilde{\nu}) - 2\sigma_{1\leftarrow0}(\tilde{\nu})$, where $\sigma_{2\leftarrow1}$ is equal to the cross section for the transition connecting the first and the second excited vibrational states and $\sigma_{1\leftarrow0}$ refers to the cross section of the fundamental vibrational transition. Because of this connection with the fundamental and the "hot" $v = 1$ to $v = 2$ transitions of the stretching modes, it is possible to make a reliable assignment of the two spectral amplitudes, $A_1(\tilde{\nu})$ and $A_2(\tilde{\nu})$, to the two coexisting ethanolamine molecules that are IR active in the stretching spectral region. This is because the anharmonicity between the cross sections, $\sigma_{2\leftarrow1}$ and $\sigma_{1\leftarrow0}$, can be deduced from the frequency spacing of the absorptive and bleaching/emissive peaks contributing to $A_i(\tilde{\nu})$. For component 2 associated with a time constant of 1.2 ps, an anharmonic shift, Δ_{NH}, of 160 cm^{-1} can be determined while it amounts to $\Delta_{OH} = 250\,cm^{-1}$ for the component 1 characterized by the 0.45 ps time constant.

Laenen *et al.* [41] reported transient spectral hole burning data for liquid ethanol using picosecond IR pulses. They were able to bleach the OH-stretching fundamental transition of CH_3CH_2OH at 3330 cm^{-1} and observed a $v = 1$ to $v = 2$ induced absorption at 3100 cm^{-1}. These numbers suggest an anharmonic shift for the OH-mode of ethanol of 230 cm^{-1}, *i.e.* in very good agreement with the anharmonic shift subtracted from the spectral amplitude, $A_1(\tilde{\nu})$. Therefore, we conclude that component 1 is brought about by the OH-vibrator of the EA-OH species. Furthermore, we can conclude that the vibrational lifetime of the OH-stretching vibration of $D_2NCH_2CH_2OH$ in ethanolamine-d3 amounts to 450 fs. For comparison, the vibrational lifetime of the $v = 1$ OH stretching state in liquid ethanol was determined by Bakker and coworkers [3] to 400 fs, which is also in full accord with the OH-lifetime deduced here for EA-OH in liquid ethanolamine-d3.

Having unraveled the vibrational dynamics of the hydroxyl oscillator of ethanolamine, we now focus on the origin of component 2. We surmise that it is due to the remaining NH-oscillator of the other species, namely the EA-NH molecule. From the frequency difference of the absorptive and bleaching/emissive peaks of $A_2(\tilde{\nu})$ an anharmonic shift of 170 cm^{-1} is obtained (see Fig. 5a). Bethomieu and Sandorfy investigated the fundamental and overtone transitions of a variety of amines [42]. For diethylamine dissolved in carbon tetrachloride, they identified the fundamental NH transition at 3332 cm^{-1} while the first overtone was discovered at 6477 cm^{-1}. These numbers suggest an anharmonic shift of 187 cm^{-1}, which indeed compares favorably with the value deduced above from $A_2(\tilde{\nu})$. Therefore, we are led to conclude that component 2 originates from the NH-oscillator of $HNDCH_2CH_2OD$ in ethanolamine-d3. The lifetime of its $v = 1$ excited state relaxes with a time constant of 1.2 ps.

Finally, the origin of the spectral amplitude, $A_3(\tilde{\nu})$, needs to be clarified. It is associated with a time constant of 5 ps and its magnitude is about one order of magnitude smaller than those of two fast components discussed so far. $A_3(\tilde{\nu})$ contains a negative going peak that coincides precisely with the sharper NH-stretching fundamental seen in the FTIR at 3309 cm^{-1}. This suggests that the third component is also due to the EA-NH molecules. $A_3(\tilde{\nu})$ also exhibits an additional positive going peak at 3160 cm^{-1}, which may then have to be assigned to the transient absorption of the NH-stretching mode that is again anharmonically shifted by roughly 170 cm^{-1}. However, in contrast to the features seen in $A_2(\tilde{\nu})$, the bandwidths of these two peaks are much smaller,

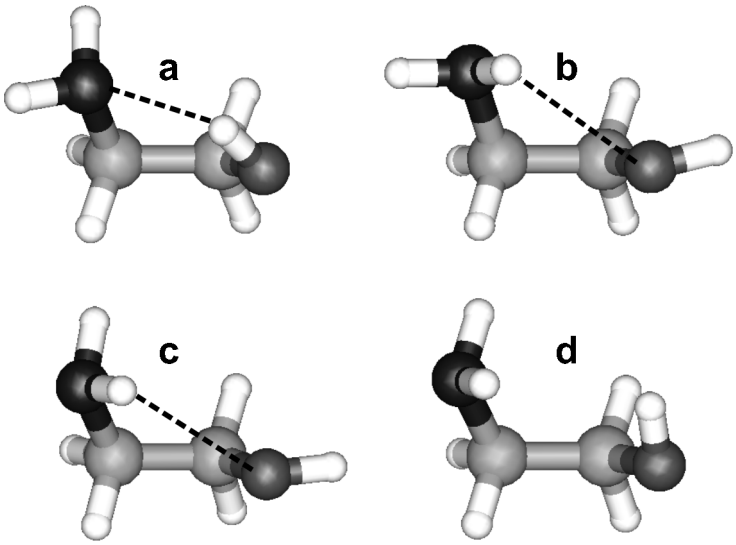

Fig. 6. DFT-optimized structures of ethanolamine in the g'Gg' (**a**), gGt (**b**), tGt (**c**), and the tGg' (**d**) conformation.

indicating that they possibly originate from an EA-NH species, that is spectroscopically distinct from that associated with the 1.2-ps relaxation process. The smaller bandwidths in combination with the longer time constant as compared to the second component implies that $A_3(\tilde{\nu})$ might be caused by NH-stretching oscillators of the EA-NH molecules, which are engaged in weaker hydrogen-bonding or no H-bonding at all. Note, that both narrow features seen in Fig. 5b ride on top of a slowly varying background that is reminiscent of the spectrum of the hot sample. Apparently, the signal-to-noise ratio of the data is not sufficiently high for the global fitting analysis to fully separate the heating dynamics from these "free" NH-stretching vibrational relaxation dynamics.

Further information about the nature of hydrogen bonds in liquid ethanolamine comes from molecular dynamics (MD) simulations [32,33,43,44]. There are basically four different types of H-bonds that can be distinguished in the neat liquid namely, those involving the hydroxyl group as the hydrogen donor (*i.e.* OH···O and OH···N configurations) and those where the amino group serves as the H-donor (*i.e.* NH···O and NH···N configurations). All of these H-bonds can occur at the intramolecular and intermolecular level.

In the gas phase, the gauche conformation about the central carbon-carbon single bond that enables an intramolecular OH···N-contact is the most stable structure of the ethanolamine molecule. In the Pople notation [45], the sequence of the three dihedral angles (lp-NH_2-CH_2-CH_2-O-H, lp = lone pair) for this conformation is g'Gg'. At the DFT-level RI-BP/aug-TZVPP/TZV-J, the intramolecular OH···N-bond distance is 2.184 Å and the OH···N-bond angle is 18.2° (see also Fig. 6a). The most stable structures enabling an intramolecular NH···O-contact are the gGt and the tGt conformers, which are nearly degenerate at the same level of theory. The NH···O-bridge is 2.526 Å

and 2.592 Å in length with an angle of 20.4° and 19.9° for gGt and tGt, respectively (*cf*. Fig. 6b,c).

Recently, MD-simulations have been carried out for the neat liquid by da Silva *et al.* [33] using a force field that has been fitted to conformer energies as well as internal rotational barriers obtained from electronic structure calculations on the monomer. These MD simulations reveal that upon entering the liquid phase the g'Gg' conformer no longer prevails and that instead the tGg' conformer (see Fig. 6d) is populated the most. This surprising finding can only be rationalized by a higher propensity of the ethanolamine molecule to formation of more stable intermolecular hydrogen bonding patterns to nearest neighbors upon sacrificing the intramolecular H-bond contacts and adoption of the tGg' conformer. Indeed, radial distribution functions for the four H-bond configurations obtained from MD simulations of the neat liquid demonstrate that NH···O and NH···N-contact are about equally likely [33]. It could very well be that the small 5-ps component observed in the fs-MIR pump-probe experiments reported here is brought about by some small remaining population of intramolecular H-bond contacts involving the amino group as donor. More sophisticated experiments including femtosecond 2-dimensional infrared (2DIR) spectroscopy [46–53] in combination with more elaborate molecular dynamics simulations are required to solve this interesting aspect.

In summary, we have presented the first MIR pump-probe studies aimed at unraveling the vibrational relaxation dynamics in liquid ethanolamine. The molecules of this intriguing liquid contain both, a very strong hydrogen-bond donor (the hydroxyl group) and a very strong hydrogen-bond acceptor (the amino group). The dynamics of NH- and OH stretching relaxation were separated spectroscopically through partial isotope labeling and high dilution of the two mono-hydrogenated ethanolamine species in the fully deuterated ethanolamine solvent.

It turned out that the OH-stretching relaxation occurs about a factor of three faster than the NH-stretching relaxation. Just like in neat liquid alcohols, we believe that for both modes the relaxation proceeds through the energetically nearby $v = 1$ CH-stretching state with the energy mismatch of about 450 cm^{-1} (see Fig. 1) being compensated for by the phonons of the liquid. This VER mechanism is purely mechanical and is defined by the cubic anharmonic couplings between the nuclear degrees of freedom of the solute and the solvent bath. It is important to emphasize that this magnitude of the energy gap between the upper (initial) and lower (final) vibrational states of the vibrationally relaxing solute is identical for the two stretching modes. Furthermore, also the chemical bonding situation and the relative distances between OH and NH bonds on the one hand and the energy accepting CH bonds on the other are almost identical suggesting that also the anharmonic solute bath couplings are similar. Nevertheless, the time scales for the OH and NH stretching relaxation are very different, which highlights the importance of the hydrogen-bond strengths and the H-bond structural details for vibrational energy relaxation dynamics in the random networks of associated liquids such as water, amines, and aminoalcohols. Further experiments including 2DIR experiments and MIR pump probe studies over as wide a range of thermodynamic conditions ranging from the liquid to the supercritical phase of ethanolamine are underway to elucidate in more detail the interplay between VER and vibrational spectral diffusion in this fascinating molecular liquid.

Acknowledgement

We are deeply grateful to Horst Hippler for his continuing support over the many years. We consider ourselves fortunate to have enjoyed his enthusiasm for science and his experienced mentorship during our time in Karlsruhe. Financial support by the Deutsche Forschungsgemeinschaft through the Collaborative Research Centers SFB 813 "Chemistry at Spin Centers" and SFB 624 "Functional Chemical Templates" as well as through Grant DFG VO 593/6-1 is gratefully acknowledged.

References

1. E. T. J. Nibbering and T. Elsaesser, Chem. Rev. **104** (2004) 1887.
2. T. Elsaesser and H. J. Bakker (Eds.), *Ultrafast Hydrogen Bonding Dynamics and Proton Transfer Processes in the Condensed Phase*, Kluwer Academic Publisher, Dordrecht, 2003.
3. A. J. Lock, S. Woutersen, and H. J. Bakker, J. Phys. Chem. A **105** (2001) 1238.
4. S. Woutersen, U. Emmerich, and H. J. Bakker, Science **278** (1997) 658.
5. S. Ashihara, N. Huse, A. Espagne, E. T. J. Nibbering, and T. Elsaesser, J. Phys. Chem. A **111** (2007) 743.
6. J. R. Schmidt, S. T. Roberts, J. J. Loparo, A. Tokmakoff, M. D. Fayer, and J. L. Skinner, Chem. Phys. **341** (2007) 143.
7. C. J. Fecko, J. D. Eaves, J. J. Loparo, A. Tokmakoff, and P. L. Geissler, Science **301** (2003) 1698.
8. S. Woutersen and H. J. Bakker, Nature **402** (1999) 507.
9. M. L. Cowan, B. D. Bruner, N. Huse, J. R. Dwyer, B. Chugh, E. T. J. Nibbering, T. Elsaesser, and R. J. D. Miller, Nature **434** (2005) 199.
10. T. L. C. Jansen, B. M. Auer, M. Yang, and J. L. Skinner, J. Chem. Phys. **132** (2010) 224503.
11. S. Knop, T. L. Jansen, J. Lindner, and P. Vöhringer, Phys. Chem. Chem. Phys. **13** (2011) 4641.
12. J. Seehusen, J. Lindner, D. Schwarzer, and P. Vöhringer, Phys. Chem. Chem. Phys. **11** (2009) 8484.
13. C. P. Lawrence and J. L. Skinner, J. Chem. Phys. **117** (2002) 8847.
14. C. P. Lawrence and J. L. Skinner, J. Chem. Phys. **117** (2002) 5827.
15. C. J. Fecko, J. J. Loparo, S. T. Roberts, and A. Tokmakoff, J. Chem. Phys. **122** (2005) 054506.
16. M. F. Kropman, H. K. Nienhuys, S. Woutersen, and H. J. Bakker, J. Phys. Chem. **105** (2001) 4622.
17. T. Schäfer, J. Lindner, P. Vöhringer, and D. Schwarzer, J. Chem. Phys. **130** (2009) 224502.
18. D. Schwarzer, J. Lindner, and P. Vöhringer, J. Phys. Chem. A **110** (2006) 2858.
19. D. Schwarzer, J. Lindner, and P. Vöhringer, J. Chem. Phys. **123** (2005) 161105.
20. R. Rey, K. B. Møller, and J. T. Hynes, J. Phys. Chem. A **106** (2002) 11993.
21. J. Lindner, D. Cringus, M. S. Pshenichnikov, and P. Vöhringer, Chem. Phys. **341** (2007) 326.
22. J. Lindner, P. Vöhringer, M. S. Pshenichnikov, D. Cringus, D. A. Wiersma, and M. Mostovoy, Chem. Phys. Lett. **421** (2006) 329.
23. N. Huse, S. Ashihara, E. T. J. Nibbering, and T. Elsaesser, Chem. Phys. Lett. **404** (2005) 389.
24. C. P. Lawrence and J. L. Skinner, J. Chem. Phys. **119** (2003) 3840.
25. V. M. Kenkre, A. Tokmakoff, and M. D. Fayer, J. Chem. Phys. **101** (1994) 10618.
26. K. Winkler, J. Lindner, and P. Vöhringer, Phys. Chem. Chem. Phys. **4** (2002) 2144.
27. K. Winkler, J. Lindner, H. Bürsing, and P. Vöhringer, J. Chem. Phys. **113** (2000) 4674.
28. P. Vöhringer, R. A. Westervelt, T. S. Yang, D. C. Arnett, M. J. Feldstein, and N. F. Scherer, J. Raman Spectr. **26** (1995) 535.
29. T. Schäfer, D. Schwarzer, J. Lindner, and P. Vöhringer, J. Chem. Phys. **128** (2008) 064502.
30. R. C. Weast (Ed.), *CRC Handbook of Chemistry and Physics*, CRC Press, Boca Raton, 1983.
31. J. Alejandre, J. L. Rivera, M. A. Mora, and V. de la Garza, J. Phys. Chem. B **104** (2000) 1332.
32. A. V. Gubskaya and P. G. Kusalik, J. Phys. Chem. A **108** (2004) 7151.

33. E. F. da Silva, T. Kuznetsova, B. Kvamme, and K. M. Merz, J. Phys. Chem. B **111** (2007) 3695.
34. J. K. Button, K. E. Gubbins, H. Tanaka, and K. Nakanishi, Fluid Phase Equilib. **116** (1996) 320.
35. P. J. Krueger and H. D. Mettee, Can. J. Chem. **43** (1965) 2970.
36. R. E. Penn and R. F. Curl Jr., J. Chem. Phys. **55** (1971) 651.
37. C. F. P. Silva, M. L. T. S. Duarte, and R. Fausto, J. Mol. Struct. **482–483** (1999) 591.
38. A. Kandratsenka, D. Schwarzer, and P. Vöhringer, J. Chem. Phys. **128** (2008) 244510.
39. C. P. Lawrence and J. L. Skinner, Chem. Phys. Lett. **369** (2003) 472.
40. J. B. Asbury, T. Steinel, and M. D. Fayer, J. Phys. Chem. B **108** (2004) 6544.
41. R. Laenen, C. Rauscher, and K. Simeonidis, J. Chem. Phys. **110** (1999) 5814.
42. C. Berthomieu and C. Sandorfy, J. Mol. Spectr. **15** (1965) 15.
43. J. Alejandre, J. L. Rivera, M. A. Mora, and V. de la Garza, J. Phys. Chem. B **104** (2000) 1332.
44. J. K. Button, K. E. Gubbins, H. Tanaka, and K. Nakanishi, Fluid Phase Equilibr. **116** (1996) 320.
45. L. Radom, W. A. Lathan, W. J. Hehre, and J. A. Pople, J. Am. Chem. Soc. **95** (1973) 693.
46. P. Hamm, M. H. Lim, and R. M. Hochstrasser, J. Phys. Chem. B **102** (1998) 6123.
47. S. Woutersen and P. Hamm, J. Phys. Cond. Matt. **14** (2002) R1035.
48. M. Khalil, N. Demirdoven, and A. Tokmakoff, J. Phys. Chem. A **107** (2003) 5258.
49. J. J. Loparo, S. T. Roberts, and A. Tokmakoff, J. Chem. Phys. **125** (2006) 194521.
50. J. Zheng, K. Kwak, and M. D. Fayer, Acc. Chem. Res. **40** (2007) 75.
51. V. Cervetto, J. Helbing, J. Bredenbeck, and P. Hamm, J. Chem. Phys. **121** (2004) 5935.
52. J. Bredenbeck, J. Helbing, C. Kolano, and P. Hamm, ChemPhysChem **8** (2007) 1747.
53. M. Olschewski, S. Knop, J. Seehusen, J. Lindner, and P. Vöhringer, J. Phys. Chem. A **115** (2011) 1210.